The effect of suffusion on physical properties and mechanical behavior of granular soils

C.D. Nguyen, Nadia Benahmed, P. Philippe, E. Andò, L. Sibille

Author produced version of the communication presented at the 9th International Conference on Scour and Erosion (ICSE 2018), November 5-8, 2018, Taipei, Taiwan. Available at https://www.taylorfrancis.com/books/9780429667794 ISBN 9780429667794

The effect of suffusion on physical properties and mechanical behavior of granular soils

C.D. Nguyen; N. Benahmed & P. Philippe
Research Unit RECOVER – Irstea, Aix-en-Provence, France

E. Andò & L. Sibille
Univ. Grenoble Alpes, CNRS, Grenoble INP, 3SR, F-38000 Grenoble, France

ABSTRACT: Internal erosion is a complex phenomenon, which is a main problem for the long-term stability of earth hydraulic structure impacted by seepage. One particular phenomenon of internal erosion, the migration of the finest soil particles through the surrounding soil matrix formed by the granular skeleton, is called suffusion. The occurrence of suffusion usually causes modifications of the microstructure and changes in the physical, hydraulic and mechanical properties of the soil. The mechanism of suffusion development and its consequences on the mechanical behavior are usually addressed at a macroscopic scale in experimental analysis while they most probably arise from microscopic processes. In this paper, the investigation of suffusion development and mechanical properties of eroded soil are linked to the microscopic scale. For this purpose, suffusion tests are firstly performed on granular soil sample using a newly developed erosion permeameter, and then subjected to a mechanical loading; while high resolution x-ray computed tomography is used to capture the micro-structural evolution during the erosion process.
The results obtained from x-ray CT analyze show that the erosion process is highly heterogeneous in term of fine content, void ratio and inter-granular void ratio, with the presence of random preferential flow paths. The presence of shear deformation and non-uniform volumetric strain in the sample after suffusion process are also remarkable. These features may cause counterintuitive results on the mechanical behavior deduced from an average stress-strain in triaxial test for eroded soil.

1 INTRODUCTION

Internal erosion, one of the main causes of dikes, levees, and embankment dams failures (Foster et al., 2000) is worldwide recognized as a complex phenomenon, for which four basic mechanisms have been identified: backward erosion, contact erosion, concentrated leak erosion, and suffusion (Bonelli, 2013). In this study, an emphasis is put on the latter. At particle-scale, suffusion stands for both the erosion and the migration under seepage flow of the finest soil particles within the surrounding static soil skeleton formed mainly of large grains. Suffusion has been studied by several researchers based on experimental approaches (Kenney & Lau, 1985; Skempton & Brogan, 1994). From results in literature and as will be highlighted by additional findings of the present investigation, the following general observations can be made: (*i*) erosion of fine particles seems heterogeneous, which may help the development of preferential flow paths; (*ii*) during the suffusion process, blockage or washout of fine particles can occur, giving rise to comparatively looser and denser zones; (*iii*) erosion of soil grains lead to the modification of the soil microstructure (fines loss, skeleton settlements) with substantial changes in some key physical properties (soil texture, porosity, etc.). This change of microstructure may substantially modify the mechanical behavior of the eroded soil. However, the way how the suffusion develops within a soil sample and its subsequent consequences on the mechanical behavior remains to be identified, despite recent progress. In particular, a number of issues remain unresolved: what is the space-time distribution of suffusion within the soil? Are there some specific locations where clogging or deformation occurs more intensively? How related microstructure changes can affect the mechanical response of eroded soils? However, these problems that most probably arise from microscopic processes are usually addressed at a macroscopic scale in usual experimental analysis. In that respect, regarding the impact of suffusion on the soil mechanical behavior, there is no universally accepted outcome, as for instance in Chang's study (Chang & Zhang, 2011), where it is

concluded that the shear strength of eroded soil decreases compared to non-eroded soil, while Xiao & Shwiyhat (2012) have come to the opposite conclusion. This fact might be due to a lack of clear information about the evolution of the soil microstructure during suffusion, as well as to the consequence of not taking into account the resulting changes of the predominant parameters such as void ratios and fines content.

In order to gain understanding of the elementary mechanisms of suffusion at the microscopic scale and to improve the interpretation of mechanical tests on eroded soils, suffusion experiments were performed on granular soil samples under different hydraulic gradients using a newly developed erosion permeameter. High resolution x-ray computed tomography was used to capture the micro-structural evolution during the erosion process. Distributions of the void ratios (overall and inter-granular) and of the fines content were specifically investigated. Thereafter, triaxial compression tests were carried out on both the eroded samples and "intact" ones (not eroded) having the same initial conditions in terms of density and fines content. The obtained mechanical results were interpreted in the light of the complementary analysis resulting from the microscale investigations using the x-ray CT.

2 EXPERIMENTAL METHOD

2.1 *Test materials*

The soil used in this study is obtained by mixing two silica sands (Hostun sand) with varying particle sizes, and sub-angular to angular grains shape. The coarse grains HN 1/2.5 (D_{50} = 1700 µm) works as the host sand while the fine particles HN 34 (D_{50} = 210 µm) are the erodible particles. With a fine content of 25% by mass (named FC25), the mixture studied in this paper is described as a poorly graded sand. The grains size distributions curves of the two sands and their mixture are shown in Figure 1. The

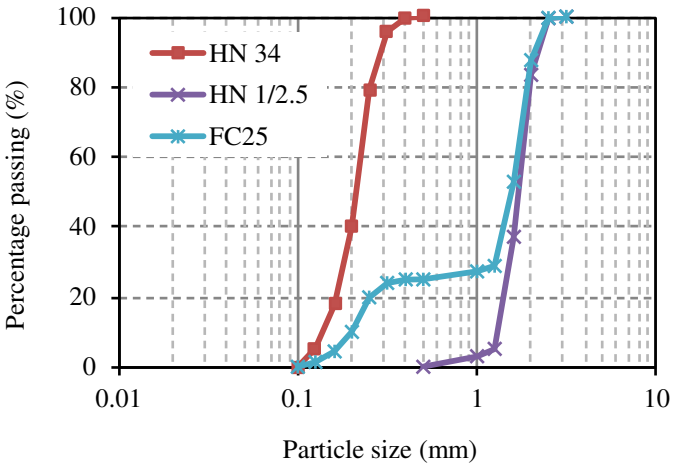

Figure 1. Grain size distribution curves of the two Hostun sands and their mixture.

physical properties of the test soil are summarized in Table 1.

According to the geometric criteria related to the assessment of internal stability of soil proposed by Kézdi (1979), Kenny & Lau (1985, 1986), Wan & Fell (2008), the used soil is evaluated as vulnerable to internal erosion. Therefore, erosion occurs once the hydraulic gradient reaches a critical value.

Table 1. Sand particles size distributions parameters.

Properties	HN 34	HN 1/2.5	FC25
Specific gravity, ρ_s	2.65	2.65	2.65
Minimum particle size D_0 (mm)	0.1	0.63	0.1
Maximum particle size D_{100} (mm)	0.5	2.5	2.5
Median particle size, D_{50} (mm)	0.21	1.7	1.6
D'_{15}/d'_{85}	-	-	5
$(H/F)_{min}$	-	-	0.12
$h' = D_{90}/D_{60}$	-	-	1.24
$h'' = D_{90}/D_{15}$	-	-	9.13

2.2 *Description of suffusion test*

2.2.1 *Permeameter device and sample preparation*

The experimental set up used in this study (Figure 2) involves a plexiglas cylinder (erosion cell) of 70 mm internal diameter and 140 mm length, whose design consists of two half cylinders assembled together in order to allow recovering the sample after the erosion test.

The cell is fixed between an upper and a lower base by using 3 tie rods between these two bases. The upper base is connected to a pump, itself connected to a water supply system while the lower base is connected to a fine particles collector.

To reduce the formation of large seepage channels along the boundary between the sample and the cylinder, a rough transparent plastic sheet was set against the inside wall of the cell before sample preparation.

A moist tamping method is used to reconstitute a homogeneous soil specimen. Particular care was taken to avoid any potential segregation. The soil is compacted in 7 layers, each layer being 20 mm thick. The target initial relative density of the specimen is 40% (semi dense soil).

The soil sample is placed above a layer consisting of 12 mm single-sized glass beads (4 mm diameter). This latter is comprised between two steel mesh screens to prevent the movement of the glass beads during the test. In the top of the cell, the same glass beads layer sandwiched between two steel screens is placed for the purpose of breaking up the incoming flow to ensure a uniform water flow at the inlet of the specimen.

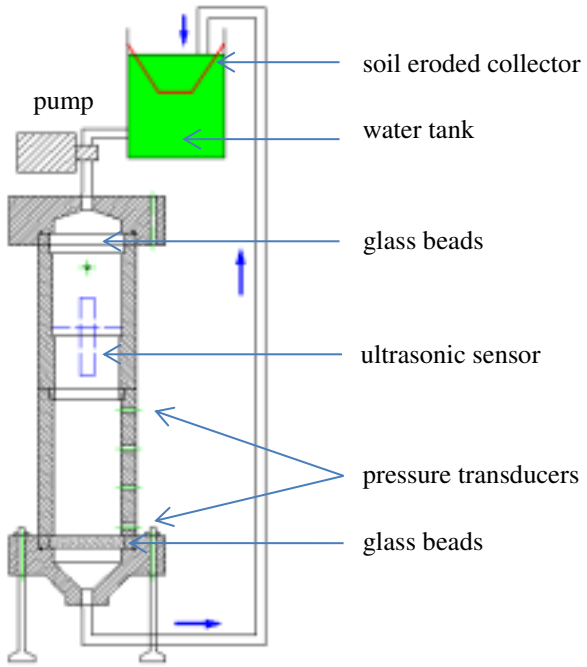

Figure 2. Schematic diagram of experimental system.

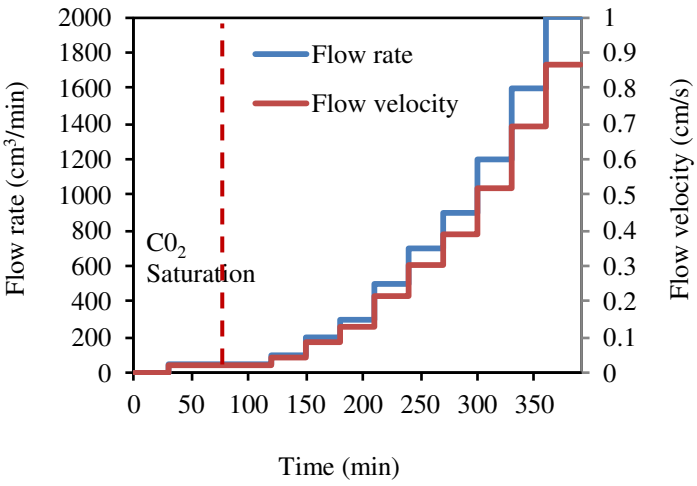

Figure 3. Illustration of increasing flow rate during the suffusion test.

The variation in water pressure within the specimen is measured by 2 sensors at 2 different depths, 20 mm and 120 mm, whose values are therefore used to calculate the average hydraulic gradient imposed across the specimen. Any height variation of the test specimen as a result of mass loss during the suffusion test is measured continuously by an axial deformation immersible sensor. Washed-out/trapped fine particles are regularly collected at the outlet in order to measure the eroded mass and further estimate the erosion rate during the test.

2.3 *Erosion test procedure*

The soil specimen is subjected to unidirectional seepage flow. Before carrying out the erosion test, the specimen was first saturated. To do this, carbon dioxide was first slowly flushed into the specimen from the bottom to displace the interstitial air, then followed by de-aired water at a very slow rate. The entire saturation process requires approximatively 1 hour. During this stage, some fine particles loss is observed.

To perform the erosion test, the flow rate is reversed from upward to downward and increased in stages to the final value. The variation in water pressure within the specimen is measured by 2 sensors at 2 different depths, 20 mm and 120 mm, whose values are therefore used to calculate the average hydraulic gradient imposed across the specimen. Any height variation of the test specimen as a result of mass loss and settlement during the suffusion test is measured continuously by an axial deformation submersible sensor. Washed-out/trapped fine particles are regularly collected at the outlet in order to measure the eroded mass and further estimate the erosion rate during the test

The initially imposed flow rate is 0.05 cm/s which gives a hydraulic gradient in the order of 0.05-0.1. The flow rate is increased at approximately the same increments. Each step lasts 30 minutes to ensure the completion of the internal erosion, *i.e.*, still there is no more removal of fine particles from the sample. A typical flow rate increasing procedure is shown in Figure 3. The eroded soil (*i.e.* fine particles) is collected by the soil collector at the end of each stage, oven-dried and weighted to estimate the erosion rate. The suffusion test is stopped when the flow rate reaches the target value.

Once the internal erosion process completed, the mechanical behavior of the eroded soil is investigated by performing triaxial compression tests. In the present case, the eroded specimen is transferred to a conventional triaxial cell, without disturbing their microstructure resulting from the erosion process, to characterize their mechanical behavior. The technique, based on freezing and de-freezing of the specimen, is not described in this paper. More detailed descriptions will be given in forthcoming publications.

2.4 *Triaxial test*

A fully computed controlled Dynamic Triaxial System from Wykehan Farrance was used. Drained and undrained triaxial compression tests at a constant strain rate of 1% per minute were carried out to investigate the stress-strain behavior of the soil beforehand subjected to internal erosion.

2.5 *Suffusion test with in-operando X-ray tomography*

In this study, the suffusion test in-operando x-ray tomography technics is used to capture the microstructure evolution induced by the suffusion process. This non-invasive scanning method is known to be very well adapted to visualize internal microstructural geometry within a volume of material. Based on contrast in x-ray absorption of the different components of the system, a 3D image is reconstructed

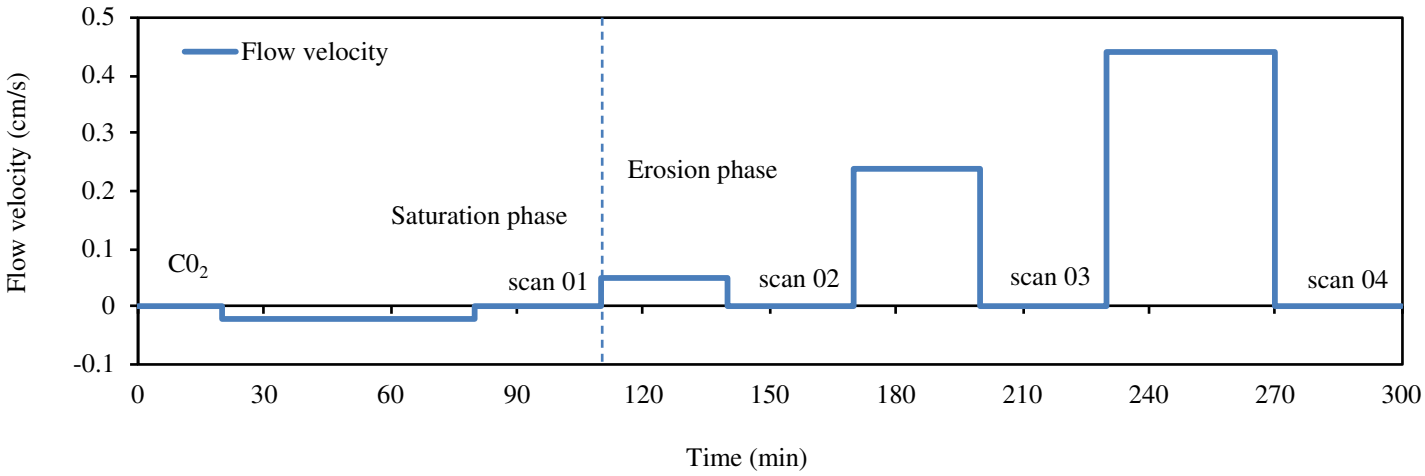

Figure 4. Application of the flow rate by step and location of the 4 successive scans.

at a resolution typically ranging from one hundred micrometers to one millimeter in voxel size (Desrues, 1996; Hasn, 2010; Hasan, 2010). In the more specific field of internal erosion, recent works by Homberg (2012), Fonseca (2014), and Dumberry (2017) have used x-ray CT.

Here, a similar suffusion test procedure regarding sample preparation and seepage induced suffusion test is performed on the same soil as presented in session 2.1. The voxel size of the x-ray CT reconstructed images is 90 µm that corresponds to $0.43d_{50}$ and $0.053D_{50}$ regarding the fine and coarse grains respectively (d_{50} and D_{50} are the median particle size of fines and coarse grains, respectively). Thus only the coarse grains can be identified individually with this resolution, while not the fine particles.

Due to experimental technical limitations in terms of time, the number of constant flow rate steps is reduced. At the end of each step, an x-ray scan of the tested sample is performed in-operando while the eroded mass is collected and later weighted after oven drying. 4 scans were performed in the present test, corresponding to 4 successive soil states during the step by step increasing flow velocity depicted in Figure 4.

The description of the x-ray device and of the image processing are not presented here but will be detailed in a forthcoming paper. The vertical sections in the median plane of each scan are presented in Figure 5 using a color map for the filling rate of fine particles in the inter-grains pores. As expected from sample preparation method by moist tamping, scan 01 and scan 02 reveal a roughly homogeneous distribution of fines content concentration. Besides, they show that at low flow rate no noticeable erosion can be observed. On the contrary, in scans 03 and 04

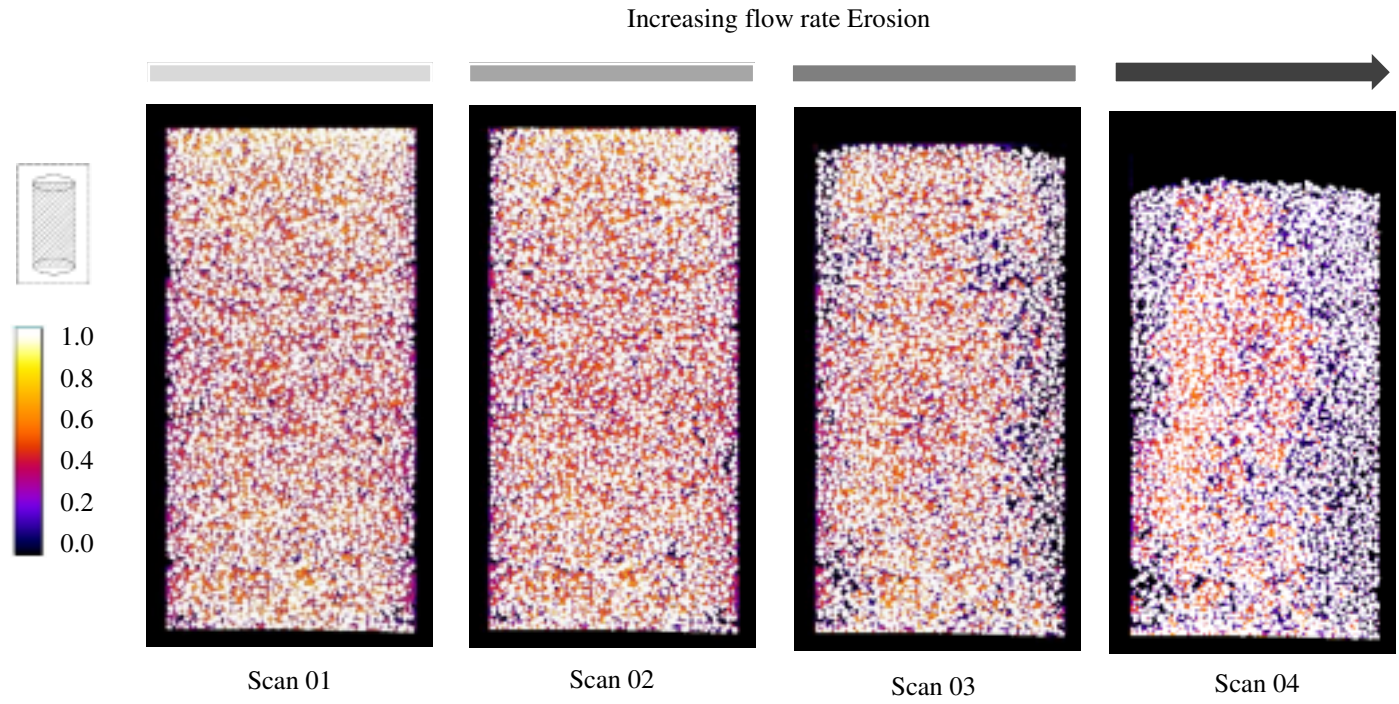

Figure 5. X-ray tomography on a bi-disperse soil sample subjected to suffusion and evidencing the erosion process heterogeneity with the formation of preferential flow paths (coarse grains appear in white and the color scale in the inter-granular voids represent the fines concentration).

where suffusion occurred, there is a significant drop in fines content, especially at the circumferential edges of the sample, indicating that most of the fine particles removal remains mainly located at the periphery of the soil sample.

3 RESULTS AND DISSCUSIONS

3.1 *On the suffusion test*

The suffusion cell is transparent which allows for the observation of the erosion mechanism from the side of the sample. A critical gradient for erosion, i_{cr}, can be defined when the first sign of erosion appears, *i.e.*, when some fine particles begin to move. Several preferential flow channels are quickly formed and expand in width with increasing flow rate. As the initial distribution of fines was approximately random, a random formation of the flow channels within the sample would be expected. However, the previous x-ray CT results suggest the occurrence of preferential flow paths and erosion channels at the sample edges. Fines are progressively fluidized in these flow channels when the flow rate increases. However, as the concentration of particles migrating through the porous structure increases, it is likely that clogging can occur whenever a local accumulation of fines develops at some locations along these channels due to collective geometrical blockage in constrictions. In addition, the loss in fine particles gradually generates slight and repetitive settlements of the coarse grains to successively achieve new stable positions. It's a complex and unpredictable phenomenon in this test of sample scale.

Typical evolutions versus time of the hydraulic gradient, the axial strain, and the fines loss are shown in Figure 6. Obviously, the increase in flow rate leads to an instantaneous increase in hydraulic gradient. Note that a linear relationship is not found between the hydraulic gradient and the flow velocity, as could be expected from Darcy's law. This is due to the simultaneous evolution of the sample's structure, as revealed for instance by the successive overall settlements observed, with substantial impact on permeability. A relaxation of the hydraulic gradient is clearly noted during each step. More precisely, the pressure sensors are installed at the sample wall and a relaxation of the pressure at the top of the sample is found while the bottom value remains almost unchanged. This is most probably related to an evolution in the microstructure, possibly located at some specific places or more uniformly scattered. Note that this relaxation is observed even if no washout of fines down to the collector occurs. Thus, redistribution of fines in the upper part of the sample is however likely to take place and could be responsible for it.

Contrarily to the hydraulic gradient, there is no visible evolution (positive or negative) of the axial strain during a constant flow velocity step, meaning that instantaneous settlements take place at each increase in flow rate but without any additional compaction meanwhile, except during the last step where a small collapse occurs (at time t ~ 325min). These instantaneous settlements are observed even before collecting any fine particles at the outlet. Note that a substantial settlement is also observed during the saturation phase, but for another reason this time related to the suppression of the initial capillary cohesion created by the moist tamping procedure.

The absence of settlement in-between two velocity flow increases suggests that most of the erosion process takes place at the very beginning of a step. One can reasonably speculate that a peak of erosion is first observed and quickly decreases with time till no more erosion occurs. Settlement by rearrange-

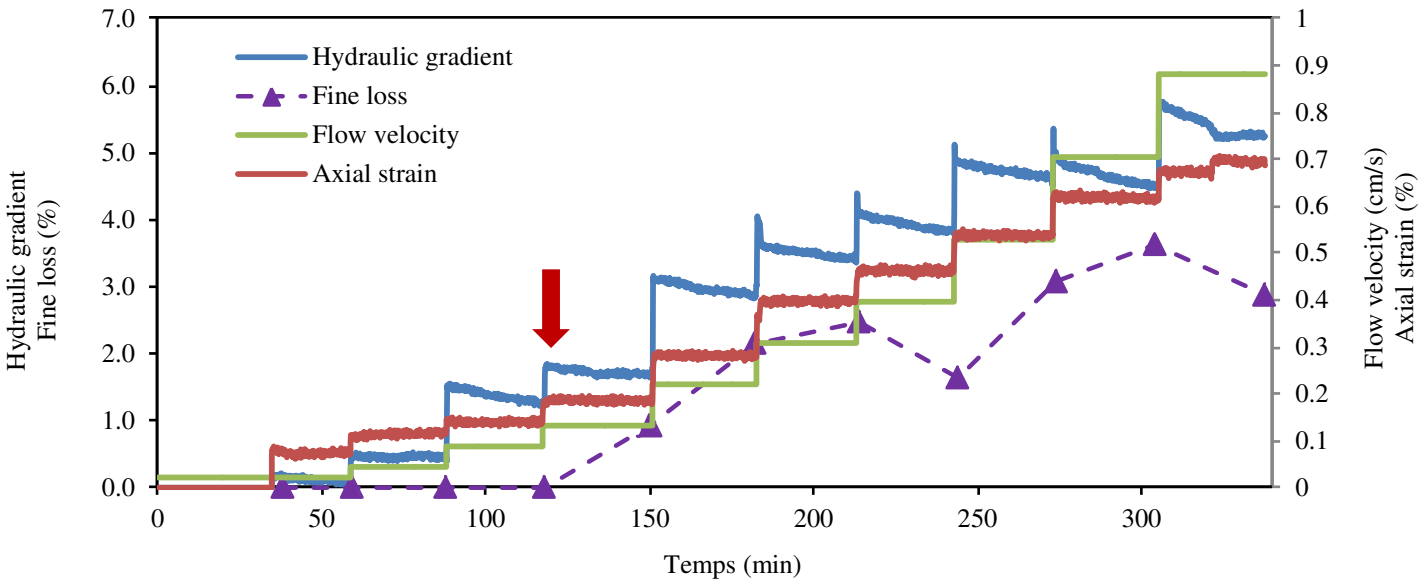

Figure 6. Hydraulic gradient, fine loss, axial strain and average flow velocity versus time. The red arrow indicates first observation of fine particles loss at the outlet.

ments of the coarse grains is consequently directly related to this fast removal of fine particles. By contrast, pressure remains sensitive to the presence of particles within the interstitial fluid, whose migration takes substantially longer. Hydraulic gradient consequently relaxes much more slowly and progressively as actually observed.

From the evolution of the fines loss over time, it can be observed that the increase in flow rate causes certainly a somewhat stronger washout of fines but not far in proportion to the flow velocity. The erosion rate seems to increase rather moderately with flow rate, especially at high flow rates where a kind of saturation occurs. In addition, the erosion rate appears to be more or less higher when a larger settlement is recorded at the beginning of the flow velocity step. This is in agreement with the presumed correlation between fines loss and overall settlement.

3.2 *Microscopic observation of the eroded soils*

From the calibrated images presented previously (Figure 5), the fines content, void ratio, and intergranular void ratio can be estimated at local positions, in each voxel. An exhaustive analysis at the microstructure scale has been carried out and will be presented elsewhere in a forthcoming paper. The main findings to be summarized here concern the appearance and development of heterogeneities in a soil sample subjected to suffusion. While only moderate variations of the local geometrical descriptors are observed along the vertical direction (flow direction), significant heterogeneities appear in the radial direction (transversally to flow direction), especially at the circumferential edges of the sample as noticed for instance in Figure 5 for scans 03 and 04 regarding fines content or also in Figure 7 where is presented the incremental deformation fields of coarse grains (deformation fields between scans 1-2, then scan 2-3, and scan 3-4).

On the deviatoric strain map, the intensity of the deviator of the strain tensor informs in particular about the presence of shear deformation. The shear appears with a low intensity in the central part of the sample after erosion (scan 03-04). On the volumetric strain map, a negative volume deformation (in blue on these images) corresponds to a decrease in volume. This decrease in volume is generally greater in the peripheral of the sample than in the center. Note

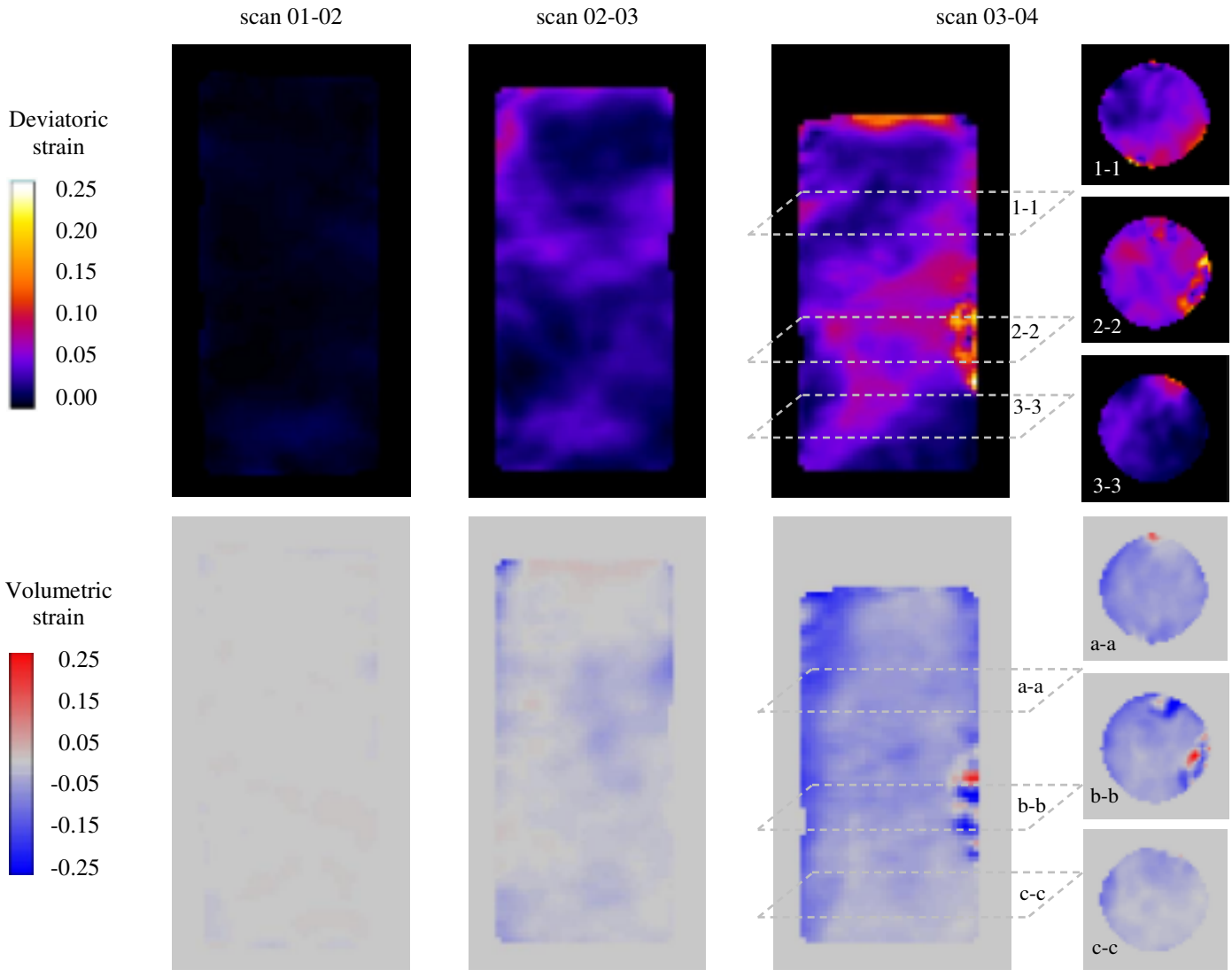

Figure 7. Map of incremental volumetric and deviatoric strain in the median plane.

that this heterogeneity between the center and the edge of the sample seems to be more specifically induced at rather low flow rates but without subsequent aggravation at higher erosion rates.

Therefore, the usual interpretation based on the physical soil properties evaluated at the sample scale may not be appropriate considering that the eroded soil sample is no longer homogeneous. The same holds for the mechanical strengths as presented in following.

3.3 *On the mechanical behavior*

The drained (D) and undrained (U) triaxial tests were comparatively conducted on a non-eroded and eroded soil, with similar initial (*i.e.,* before erosion) composition and density (FC = 25% and D_r = 40%, respectively), under an initial effective confining pressure of 100 kPa. The tested soil properties (post-consolidation in the usual triaxial test procedure) are given in Table 2. Smaller fines contents observed in the eroded samples are associated to looser specimens, with a high decrease of the relative density (D_r) and more limited changes in inter-granular void ratio (e_g).

Table 2. Summary of test conditions.

Specimen	FC (%)	D_r (%)	e	e_g	
FC25.Dr40.D	25	39.7	0.530	1.040	
FC25.Dr40.D.er	16.5	20.1	0.604	0.922	
FC25.Dr40.U		25	47.3	0.512	1.015
FC25.Dr40.U.er		16.9	7.2	0.632	0.964

D: drained test; U: Undrained test, "er" for eroded soils

One should note the non-repeatability of the erosion test which leads to different final density after erosion (D_r = 20.1 % and 7.2 %) despite the same initial conditions (D_r = 40%). This is attributed to the induced settlements which differ from one sample to another.

Figure 8 presents the stress-strain relationship with the corresponding volumetric strains evolution for the drained monotonic compression on the non-eroded and eroded soils. It can be observed that the deviator stress of an eroded soil has a similar tendency as the non-eroded soil. However, at the same strain level, the deviator stress of the eroded soil is smaller compared to that of the non-eroded soil. This is in accordance with the lower fines content and the larger global void ratio even though the denser skeleton of coarse grains (as revealed by the lower inter-granular void ratio value).

The lower drained strength of eroded soil compared to that of the non-eroded soil observed here is similar with previous findings by Muir Wood et *al.,* (2010) who concluded that internal erosion would cause lower soil strength. Furthermore, the experimental results from Chang & Zhang (2011) and Ke & Takahashi (2014) have also showed that the drained compression strength would decrease after internal erosion. However, it seems that none general conclusion can be proposed. Indeed, some results not presented here showed the opposite tendency, as also observed by Aboul Hosn et al. (2017). It is worth to notice that in the results presented in the literature, the combined effect of the fines content and the inter-granular void ratio, as well as heterogeneity was not clearly mentioned, nor taking into account.

Regarding the volumetric strains, contractive behavior is observed in both cases and the eroded soil has, marginally, a slightly smaller volumetric deformation while it is expected to exhibit a more contractive behavior, in coherence to the obtained deviatoric stress. This surprising tendency was found for other densities whose results would be published in forthcoming paper.

Figure 9 presents the stress-strain relationship for the undrained compression on the non-eroded and eroded soils. Both soils have the same stress-strain response as contractant-dilatant behavior. However, when the specimen reaches the phase transformation point, the undrained deviator stress of the eroded soil is somehow larger than that of the non-eroded soil, indicating more hardening behavior.

In the light of the observations at microscopic scale using the x-ray tomography, the reason for the differences on mechanical behavior between non-eroded and eroded soils, which is first attributed to the physical properties changes of the eroded specimen, is likely to be also due to the induced structural heterogeneities. In particular, the previous counterintuitive results regarding volumetric strains (drained behavior) might be also explained by these microstructural heterogeneities, especially by the presence of the non-uniform volumetric strains field.

Therefore, the interpretation of the eroded soil behavior based only on physical soil properties can cause certain shortcomings. The microscopic comparison of a soil sample before and after erosion process can help clarifying the understanding of suffusion process at local scale and potential impact on mechanical behavior.

4 CONCLUSIONS

This paper provides a contribution to the study of internal erosion by suffusion, with a more specific focus on the correlation between microstructural evolution during erosion process by suffusion and macro-mechanical behavior of granular soils.

A permeameter device was developed to perform suffusion tests on poorly graded soils by constant flow rate control with a continuous measurement of the induced hydraulic pressure drop between the top and bottom of the sample and the axial displacement of the upper surface of the sample. The eroded mass was also collected and measured periodically. The

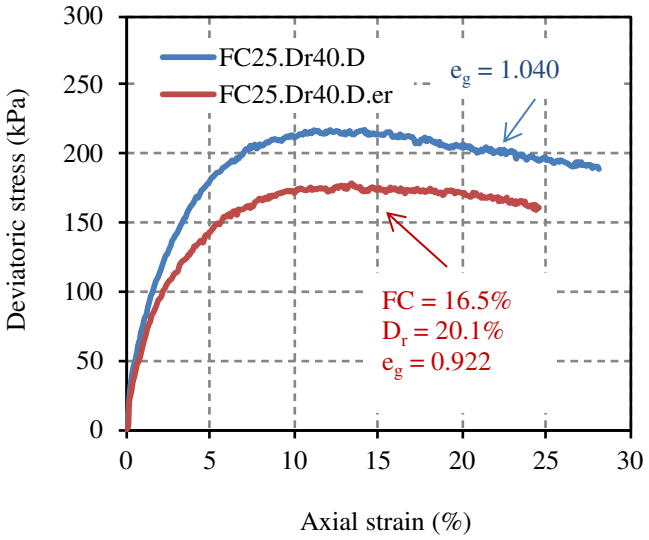

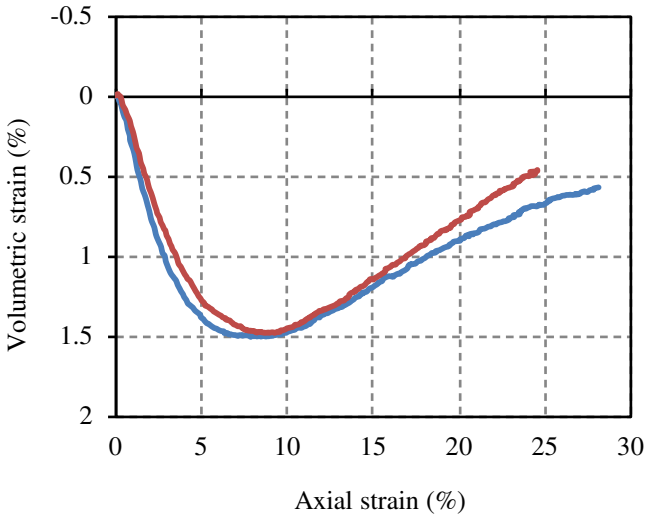

Figure 8. Drained triaxial tests on the non-eroded and eroded soils.

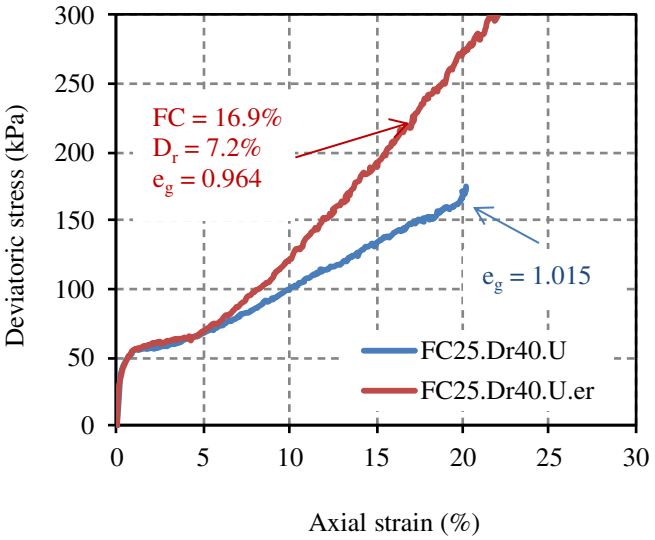

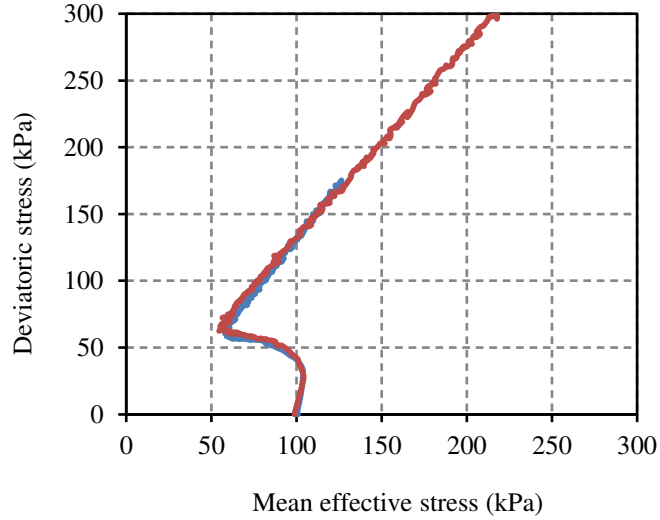

Figure 9. Undrained triaxial tests on the non-eroded and eroded soils.

mechanical consequences of internal erosion could be assessed through drained and undrained compression tests by using the triaxial apparatus on an eroded soil and its non-eroded counterpart.

For the erosion test, the random preferential flow paths and erosion channels are observed from the edges, which reveal an induced heterogeneity of the sample after erosion. The increase in flow rate leads to an increase in hydraulic gradient and causes instantaneous settlements. However, the axial strain during the application of a constant flow velocity step remains fairly constant, in contrary to what is observed in the case of hydraulic gradient. Indeed, most of wash-out process takes place in short time after changing flow rate. Accordingly, settlement is directly related to this fast removal of fine particles. In contrast, pressure remains sensitive to the presence of particles within the interstitial fluid, whose migration takes substantially longer.

By using x-ray tomography techniques, the observations of microstructural changes during the suffusion process are characterized. The heterogeneities in term of fines content distribution and inter-granular void ratio (hence, void ratio) appear in the radial direction, especially at the edges of the sample, inducing singularities in some zones. These heterogeneities have led to the presence of shear deformation and a non-uniform volumetric strain field in the sample after suffusion process.

Regarding the mechanical behavior, the soil strength of eroded soil differs from that to non-eroded soil. The erosion process could reduce (or enhance) the shear resistance of soil, depending on the combined effect of the resulted fines content, inter-granular void ratio evolution as well as the induced heterogeneities as evidenced by the x-ray tomography investigations. If the data obtained from an average stress-strain in triaxial tests could follow the common dependencies to physical soil properties for the homogeneous samples (non-eroded soils), it is however necessary to take into account other parameters for eroded soils such as the non-uniform deformation, the existing defects in the sample due to erosion, and a degree of heterogeneity that remains to be defined. These peculiar features may explain the counterintuitive results obtained on the mechanical behavior from an average stress-strain of eroded soils.

In fine, it would be now of great interest to follow the mechanisms taking place on eroded soil during

the triaxial test by using the x-ray tomography throughout the mechanical loading, to see if some localizations or bifurcations appear in the observed singularities on the eroded soil.

ACKNOWLEDGEMENTS

A funding provided by PACA region is gratefully acknowledged as well as a fruitful partnership with the engineering company SAFEGE. The support of Grenoble Alpes University through the project ERODE (programme AGIR) is also acknowledged. We thank P. Charrier and R. Aboul Hosn from Laboratoire 3SR and L.H. Luu and A. Wautier from IRSTEA for the help provided during the realization of the x-ray tomography test presented in this paper. We also would like to thank D. Marot and Y. Khidas for their fruitful discussions.

REFERENCES

Aboul Hosn, R., Nguyen, C. D., Sibille, L., Benahmed, N., & Chareyre, B. (2017, May). Microscale analysis of the effect of suffusion on soil mechanical properties. In *International Workshop on Bifurcation and Degradation in Geomaterials* (pp. 117-124). Springer, Cham.

Bonelli, S. (Ed.). (2013). *Erosion in geomechanics applied to dams and levees*. John Wiley & Sons.

Chang, D. S., & Zhang, L. M. (2011). A stress-controlled erosion apparatus for studying internal erosion in soils. *Geotechnical Testing Journal*, *34*(6), 579-589.

Desrues, J., Chambon, R., Mokni, M., & Mazerolle, F. (1996). Void ratio evolution inside shear bands in triaxial sand specimens studied by computed tomography. *Géotechnique*, *46*(3), 529-546.

Dumberry, K., Duhaime, F., & Ethier, Y. A. (2017). Erosion monitoring during core overtopping using a laboratory model with digital image correlation and X-ray microcomputed tomography. *Canadian Geotechnical Journal*, (999), 1-12.

Foster, M., Fell, R., & Spannagle, M. (2000). The statistics of embankment dam failures and accidents. *Canadian Geot.*, 37(5), 1000-1024.

Hall, S. A., Bornert, M., Desrues, J., Pannier, Y., Lenoir, N., Viggiani, G., & Bésuelle, P. (2010). Discrete and continuum analysis of localised deformation in sand using X-ray μCT and volumetric digital image correlation. *Géotechnique*, *60*(5), 315-322.

Hasan, A., & Alshibli, K. A. (2010). Experimental assessment of 3D particle-to-particle interaction within sheared sand using synchrotron microtomography. *Géotechnique*, *60*(5), 369-379.

Homberg U., Baum D., Prohaska S., Kalbe U., Witt K. J., (2012): Automatic Extraction and Analysis of Realistic Pore Structures from μCT Data for Pore Space Characterization of Graded Soil. *6th International Conference on Scour and Erosion 2012 (ICSE-6)*.

Ke, L., & Takahashi, A. (2014). Triaxial erosion test for evaluation of mechanical consequences of internal erosion. *Geotechnical Testing Journal*, *37*(2), 347-364.

Kenney, TC, & Lau, D. (1985). Internal stability of granular filters. *Canadian Geotechnical Journal*, 22(2), 215-225.

Kenney, T.C. and Lau, D. (1986) Internal Stability of Granular Filters: *Reply. Canadian Geotechnical Journal, 23*, 420-423.

Kézdi, Á. (1979). Soil physics: selected topics (Vol. 25). *Elsevier*.

Muir Wood, D., Maeda, K., & Nukudani, E. (2010). Modelling mechanical consequences of erosion. *Géotechnique*, *60*(6), 447-457

Skempton, AW, & Brogan, JM. (1994). Experiments on piping in sandy gravels. *Geotechnique*, 44(3), 449-460.

Wan, C. F., & Fell, R. (2008). Assessing the potential of internal instability and suffusion in embankment dams and their foundations. *Journal of Geotechnical and Geoenvironmental Engineering*, *134*(3), 401-407.

Xiao, Ming, & Shwiyhat, Nathan. (2012). Experimental investigation of the effects of suffusion on physical and geomechanic characteristics of sandy soils. *Geotech Testing J*, 35(6), 890-900.